

# Selective isopropylation of biphenyl to 4,4'-DIPB over mordenite (MOR) type zeolite obtained from a layered sodium silicate magadiite

T. Selvam<sup>a</sup>, G.T.P. Mabande<sup>a</sup>, W. Schwieger<sup>a,\*</sup>, Y. Sugi<sup>b</sup>, I. Toyama<sup>b</sup>, Y. Kubota<sup>b</sup>, H.-S. Lee<sup>c</sup>, and J.-H. Kim<sup>c</sup>

<sup>a</sup>*Institute of Chemical Reaction Engineering, University of Erlangen-Nürnberg, Egerlandstraße 3, D-91058 Erlangen, Germany*

<sup>b</sup>*Department of Materials Science and Technology, Faculty of Engineering, Gifu University, Gifu 501-1193, Japan*

<sup>c</sup>*Department of Chemical Technology, College of Engineering, Chonnam National University, Gwangju 500-757, South Korea*

Received 3 January 2004; accepted 6 January 2004

A mordenite (MOR) sample with submicron crystallite size (0.1  $\mu\text{m}$ ) has been synthesized by hydrothermal transformation of a layered sodium silicate magadiite (Na-magadiite) using tetraethylammonium hydroxide (TEAOH) as an intercalating agent and/or structure directing agent. The MOR sample obtained from Na-magadiite was found, by XRD and  $\text{N}_2$  adsorption measurements, to have high crystallinity and high BET surface area. However, the  $^{27}\text{Al}$  MAS NMR spectrum of the calcined MOR sample showed the presence of extra framework octahedrally coordinated aluminum. The catalytic activity of the MOR sample obtained from Na-magadiite was tested for the isopropylation of biphenyl and compared with results obtained with a commercial MOR sample with larger crystallite size (1.0  $\mu\text{m}$ ). Both samples showed comparable catalytic activity for the isopropylation of biphenyl, especially at higher temperatures. Under the reaction conditions used, the MOR sample obtained from Na-magadiite showed about 10% lower selectivity for the desired products 4,4'-DIPB and 4-IPBP compared to the commercial MOR sample. Furthermore, unexpectedly, the conversion of 4,4'-DIPB over the MOR sample obtained from Na-magadiite was significantly lower than that of the commercial MOR sample. These differences in catalytic activity might be related to the presence of extra framework octahedrally coordinated aluminum in the MOR sample obtained from Na-magadiite.

**KEY WORDS:** isopropylation; biphenyl, 4,4'-DIPB; mordenite; nanosized; Na-magadiite.

## 1. Introduction

4,4'-Dialkylbiphenyls are important monomers for the production of advanced polyester fibers, engineering plastics and liquid crystalline polymers [1]. Conventionally, the alkylation of biphenyl is carried out in the presence of catalysts such as aluminum trichloride [2] and silica–alumina catalysts [3]. These catalysts generally produce large amounts of undesired products along with less than 30% of the desired 4,4'-dialkylbiphenyls. The isopropylation of biphenyl over various zeolite catalysts is well documented in the literature [4–11]. Zeolite catalysts are attractive for several reasons: enhanced selectivity of the desired product, easy separation, reusability and most importantly they are environmentally benign materials. Among zeolite catalysts, mordenite (MOR) type zeolite possesses particularly good shape selectivity characteristics for the isopropylation of biphenyl with propylene [12–17]. In comparison to low-silica MOR catalysts, highly dealuminated MOR catalysts showed high activity and improved selectivity in the isopropylation of biphenyl.

It is well known that the crystal size has profound influence on the properties of the zeolite catalysts. Conventional zeolite catalysts normally have crystal sizes in the micrometer range. Large crystal sizes can cause heat and mass transfer problems in catalytic processes, thus reducing the performance of the catalysts. In order to meet the requirement of high effectiveness of the zeolite catalysts, there has been considerable interest in the synthesis of nanosized zeolites. One of the notable characteristics of nanosized zeolites is their shorter diffusion path length. Thus, they exhibit higher catalytic activity and coking resistance compared to conventional zeolite catalysts [18,19].

We have recently reported the hydrothermal transformation of a layered silicate, Na-magadiite, into MOR type zeolite, using TEAOH as an intercalating agent and/or structure directing agent [20,21]. MOR crystallites obtained from Na-magadiite are in the submicron (0.1  $\mu\text{m}$ ) range, much smaller than the MOR crystallites (1–15  $\mu\text{m}$ ) synthesized by conventional hydrothermal crystallization with and without the aid of organic structure directing agent (Mordenite type zeolite ( $\text{SiO}_2/\text{Al}_2\text{O}_3 = 18.7$ ) obtained from Tosoh Corporation, Tokyo, Japan) [22,23]. Very recently, the synthesis of MOR nanocrystals (62–100 nm) in the

\*To whom correspondence should be addressed.

E-mail: wilhelm.schwieger@rzmail.uni-erlangen.de

absence of organic structure directing agents has also been reported [24].

Although more than 50–90% yield of 4,4'-DIPB can be achieved in the isopropylation of biphenyl over the catalysts known so far (dealuminated H-MOR and Ce-modified H-MOR) [15,25], the use of MOR type zeolite (0.1  $\mu\text{m}$ ) obtained from Na-magadiite should lead to a reduction of diffusion limitations and an increase in conversion in comparison to the use of the above mentioned catalysts. The objective of the present study is to extend our investigation of isopropylation of biphenyl with propylene to the use of MOR type zeolite catalyst obtained from Na-magadiite. In this paper, we report the synthesis and characterization of MOR type zeolite obtained from Na-magadiite and its catalytic activity in the isopropylation of biphenyl to 4,4'-DIPB and the isomerization of 4,4'-DIPB. The results are compared with a commercial MOR sample obtained from Tosoh Corporation, Tokyo, Japan.

## 2. Experimental

### 2.1. Hydrothermal transformation of Na-magadiite into MOR type zeolite

A MOR sample with a  $\text{SiO}_2/\text{Al}_2\text{O}_3$  ratio of 13.4 was synthesized by a hydrothermal transformation of Na-magadiite. The molar composition of the Na-magadiite sample used in this study was 13.8  $\text{SiO}_2$  :  $\text{Na}_2\text{O}$  : 9.8  $\text{H}_2\text{O}$ . The hydrothermal transformation of Na-magadiite into MOR was performed as follows: Na-magadiite was added to a solution containing tetraethylammonium hydroxide (TEAOH, 30% aqueous), sodium hydroxide (99%, Fluka), potassium hydroxide (85%, Fluka) and deionized water and then the mixture was stirred for 45 min. The required amount of sodium aluminate (19.93%  $\text{Al}_2\text{O}_3$  and 19.11%  $\text{Na}_2\text{O}$ , Tricat GmbH) was then added dropwise and the stirring was continued for another 1 h. The molar composition of the reaction mixture was: 0.33  $\text{Na}_2\text{O}$  : 0.08  $\text{K}_2\text{O}$  : 0.025  $\text{Al}_2\text{O}_3$  :  $\text{SiO}_2$  : 0.35 TEAOH : 35  $\text{H}_2\text{O}$ . The resultant mixture was transferred into a Teflon-lined autoclave (50 mL) and heated at 175  $^\circ\text{C}$  for 24 h. The resultant product was collected by centrifuging at 6000 rpm, dried at room temperature and then calcined at 550  $^\circ\text{C}$  for 12 h in air. The calcined MOR sample (Na-form) was converted into its protonic form by ion-exchanging with 1 M  $\text{NH}_4\text{NO}_3$  solution at 70  $^\circ\text{C}$  for 12 h and then recalcined at 550  $^\circ\text{C}$  for 12 h. The ion-exchange procedure was repeated two times.

### 2.2. Characterization

The powder X-ray diffraction patterns were recorded on a Philips X-ray diffractometer using  $\text{CuK}_\alpha$  radiation. The range of scanning was 2–50 $^\circ$  at a rate

of 0.1 $^\circ/\text{min}^{-1}$ . The morphology and the particle size were examined by scanning electron microscopy (SEM). SEM was carried out using a JEOL JSM 6400 scanning electron microscope operated at 20 kV. The  $\text{N}_2$  adsorption measurements were obtained at 77 K using an automated nitrogen adsorption analyzer (Micromeritics, ASAP 2010). The samples were out-gassed at 300  $^\circ\text{C}$  for 3 h prior to adsorption. The total acidity of the catalysts used in this study was determined by temperature programmed desorption of ammonia ( $\text{NH}_3$ -TPD, AMI-100, Altamira). The elemental analyses of the samples were determined by Inductively Coupled Plasma Atomic Emission Spectroscopy (Perkin-Elmer 400).  $^{13}\text{C}$  CP MAS NMR and  $^{27}\text{Al}$  MAS NMR spectra of the as-synthesized samples were recorded on a Varian UNITY Inova 400 FT-NMR spectrometer. The *o*-xylene adsorption measurements were performed at 120  $^\circ\text{C}$  using a gravimetric method.

### 2.3. Catalytic experiments

In order to probe the reactivity of both internal and external acid sites of the catalysts, the catalytic cracking of aromatic compounds including cumene (IPB) and bulkier 1,3,5-TIPB were carried out on the MOR samples. The catalytic experiments were carried out in a conventional pulse reactor at 400  $^\circ\text{C}$  using 10 mg of the catalyst. Pure helium was used as the carrier gas. The products were analyzed by on-line Gas Chromatograph (Shimadzu 4C) with a FID Detector.

The isopropylation of biphenyl was carried out in a 100 mL batch reactor (SUS-316) in the temperature range of 200–350  $^\circ\text{C}$  at a propylene pressure of 0.8 MPa using the MOR sample obtained from Na-magadiite as the catalyst. For comparison, the isopropylation of biphenyl was carried out over a commercial MOR ( $\text{SiO}_2/\text{Al}_2\text{O}_3 = 18.7$ ) sample obtained from Tosoh Corporation, Tokyo, Japan. In a typical run, 50 mmol of biphenyl and 0.25 g of the catalyst were introduced into the autoclave. Prior to heating, the autoclave was purged with nitrogen and heated to attain the desired reaction temperature. After the reactor temperature was attained, propylene was introduced into the autoclave. The propylene pressure (0.8 Mpa) was kept constant over a period of 4 h. After completion of the reaction (4 h), the autoclave was cooled to room temperature. The catalyst was then filtered and washed with toluene. The reaction products were analyzed in a gas chromatograph (Shimadzu GC-14A) fitted with an Ultra-1 capillary column (HP, 25 m  $\times$  0.3 mm). The identity of the products was established by GC-MS (Shimadzu, QP 5000). The conversion and selectivity were calculated on the basis of a method reported previously [25].

### 3. Results and discussion

#### 3.1. Catalyst characterization

Physico-chemical properties of the MOR samples used in this study are given in table 1. The XRD patterns of the starting material Na-magadiite and the MOR sample obtained from Na-magadiite and the commercial MOR sample are shown in figure 1.

Table 1  
Physico-chemical properties of mordenite samples used for isopropylation of biphenyl

Sample	SiO <sub>2</sub> /Al <sub>2</sub> O <sub>3</sub> ratio	Particle size (μm)	Surface area (m <sup>2</sup> g <sup>-1</sup> )	Micro-pore volume (cm <sup>3</sup> g <sup>-1</sup> )	Acidity (μmol · g <sup>-1</sup> ) <sup>a</sup>
H-mordenite <sup>b</sup>	13.4	0.1	419	0.17	168
H-mordenite <sup>c</sup>	18.7	1	440	0.18	620

<sup>a</sup>Total acidity was determined from NH<sub>3</sub>-TPD measurements.

<sup>b</sup>Sample obtained from Na-magadiite.

<sup>c</sup>Commercial sample (Tosoh Corporation, Tokyo, Japan).

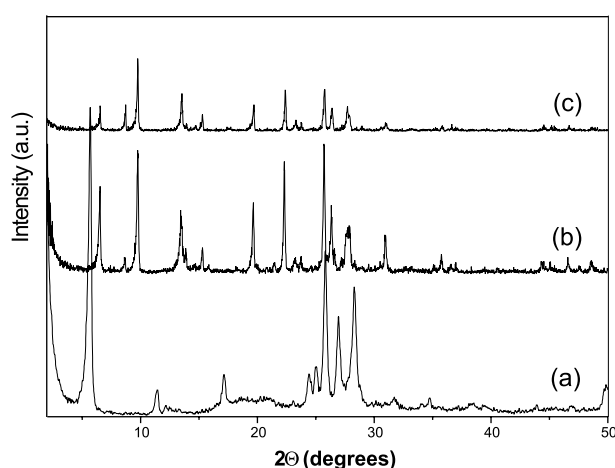


Figure 1. X-ray powder diffraction patterns of: (a) Na-magadiite, (b) MOR sample (SiO<sub>2</sub>/Al<sub>2</sub>O<sub>3</sub> = 13.4) obtained from Na-magadiite at 175 °C for 24 h [0.33 Na<sub>2</sub>O : 0.08 K<sub>2</sub>O : 0.025 Al<sub>2</sub>O<sub>3</sub> : SiO<sub>2</sub> : 0.35 TEAOH : 35 H<sub>2</sub>O] and (c) commercial mordenite sample (SiO<sub>2</sub>/Al<sub>2</sub>O<sub>3</sub> = 18.7).

The XRD pattern of Na-magadiite (curve 'a') matches well with the XRD pattern reported in the literature [26]. All the reflections are typical of Na-magadiite and indicate that the product is free from impurities. The D-spacing of Na-magadiite is 15.4 Å, which is very similar to values reported previously [26,27]. The XRD pattern of the MOR sample (curve 'b') obtained from Na-magadiite is in good agreement with the reported XRD pattern of the MOR structure [28]. The absence of additional peaks related to Na-magadiite and the high intensity of the peaks, indicate that the MOR sample is pure and highly crystalline. As far as the peak positions are concerned, the XRD pattern of the MOR sample obtained from Na-magadiite is very similar to the XRD pattern of the commercial MOR sample. However, the reflections of the commercial MOR sample are much weaker in intensity. The MOR sample obtained from Na-magadiite has a higher percentage of crystallinity (100%) in comparison to the commercial MOR sample (31%). The commercial MOR sample is synthesized in the absence of template whereas the transformation of Na-magadiite to MOR is achieved in the presence of template (TEAOH). It is well known that the hydrothermal synthesis of zeolites in the presence of templates generally yields highly crystalline material [29]. This is one of the main reasons for the difference in the percentages of crystallinity.

Figure 2 shows the SEM images of the MOR sample obtained from Na-magadiite and the commercial MOR sample. The MOR crystallites obtained from Na-magadiite are in the submicron range (0.1 μm). In general, the starting material Na-magadiite exhibits rosette-like morphology comprised of spherical aggregates of about 8–0 μm in diameter [20]. It is evident that the MOR crystallites obtained from Na-magadiite are free from agglomerates and/or impurities related to Na-magadiite. However, the SEM image of the commercial MOR sample shows crystallites which are significantly larger in size (1 μm) in comparison to the MOR crystallites obtained from Na-magadiite.

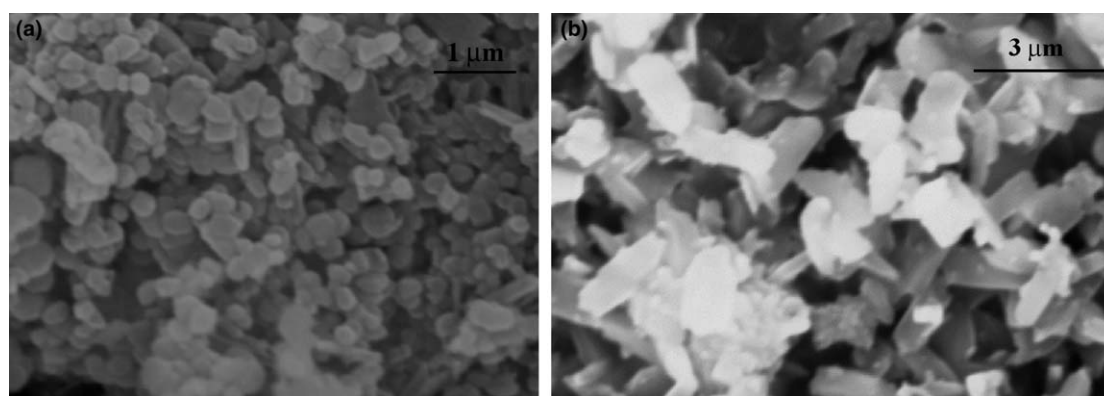


Figure 2. SEM images of: (a) mordenite sample (SiO<sub>2</sub>/Al<sub>2</sub>O<sub>3</sub> = 13.4) obtained from Na-magadiite at 175 °C for 24 h [0.33 Na<sub>2</sub>O : 0.08 K<sub>2</sub>O : 0.025 Al<sub>2</sub>O<sub>3</sub> : SiO<sub>2</sub> : 0.35 TEAOH : 35 H<sub>2</sub>O] and (b) commercial mordenite sample (SiO<sub>2</sub>/Al<sub>2</sub>O<sub>3</sub> = 18.7).

For simplicity, the MOR sample obtained from Namagadiite is referred hereafter to as the “nanosized” MOR sample.

The  $N_2$  adsorption isotherms of the nanosized MOR sample and the commercial MOR sample are shown in figure 3. Both samples show type I isotherms which are characteristic of microporous materials. The BET surface area ( $419 \text{ m}^2 \text{ g}^{-1}$ ) and micropore volume ( $0.17 \text{ cm}^3 \text{ g}^{-1}$ ) of the nanosized MOR sample are comparable to values for the commercial MOR sample (surface area,  $440 \text{ m}^2 \text{ g}^{-1}$ ; micropore volume,  $0.18 \text{ cm}^3 \text{ g}^{-1}$ ).

Since samples composed of small crystallites have a larger external surface area than those with large crystallites, the prior generally have higher adsorption capacity for organic molecules. Thus, the rate of *o*-xylene adsorption is a sensitive measure of the particle size of the catalysts. Figure 4 shows the adsorption kinetics of *o*-xylene over the nanosized MOR sample and the commercial MOR sample. As expected, the uptake of *o*-xylene over the nanosized MOR sample ( $35 \text{ mg/g}$  of

catalyst) is slightly higher than that for the commercial MOR sample ( $29 \text{ mg/g}$  of catalyst) at the end of the adsorption period of 5 min. Such high adsorption capacities for *o*-xylene are indicative of the purity of the MOR samples used in the present study.

Figure 5 shows the  $^{29}\text{Si}$ -MAS NMR spectra of the nanosized MOR sample (H-form) and the commercial MOR sample (H-form). The  $^{29}\text{Si}$ -MAS NMR spectrum of the nanosized MOR sample (curve ‘a’) exhibits a peak at  $-113.4 \text{ ppm}$  which can be assigned to Si atoms with no adjacent aluminum [Si(0Al)]. In our previous study [21], however, we observed three signals at  $-113$ ,  $-105$  and  $-99 \text{ ppm}$  for the as-synthesized nanosized MOR sample. We assigned the latter two signals to Si atoms with one adjacent aluminum atom, [Si(1Al)] and Si atoms with two adjacent aluminium atoms [Si(2Al)], respectively. However, the  $^{29}\text{Si}$ -MAS NMR spectrum of the commercial MOR sample (curve ‘b’) shows a strong signal for Si(0Al) ( $-112.5 \text{ ppm}$ ) and a poorly resolved signal for Si(1Al) ( $-106.8 \text{ ppm}$ ). The  $^{27}\text{Al}$  MAS NMR spectrum (figure 6a) of the nanosized MOR sample is composed of a strong signal at  $55.4 \text{ ppm}$  and a broad signal at  $0.4 \text{ ppm}$ . The strong signal ( $55.4 \text{ ppm}$ ) is attributed to the presence of aluminum atoms in tetrahedral coordination. The broad signal at  $0.4 \text{ ppm}$  is related to the presence of extra framework octahedrally coordinated aluminum atoms that were removed from the tetrahedral positions during the calcination process. It is important to mention here that no such extra framework aluminum species were observed in the as-synthesized nanosized MOR sample [21]. It is interesting to note that the  $^{27}\text{Al}$  MAS NMR spectrum of the commercial sample (figure 6b) shows a sharp signal at  $55.6 \text{ ppm}$  and a very weak signal at  $-1.3 \text{ ppm}$ . It appears that the commercial MOR sample has a much lower content of extra-framework species in comparison to the nanosized MOR sample. These results are further substantiated by the  $\text{NH}_3$ -TPD measurements (table 1). The  $\text{NH}_3$ -TPD studies reveal that the total acidity of the nanosized MOR sample ( $168 \mu\text{mol g}^{-1}$ ) is considerably lower in comparison to the commercial MOR sample ( $620 \mu\text{mol g}^{-1}$ ).

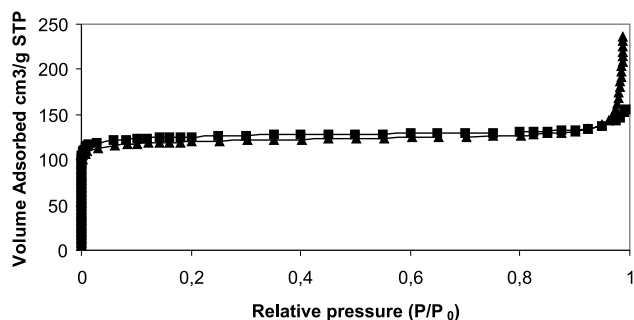


Figure 3.  $N_2$  adsorption isotherms of: nanosized mordenite sample ( $\text{SiO}_2/\text{Al}_2\text{O}_3 = 13.4$ ) ( $\blacktriangle$ ) and commercial mordenite sample ( $\blacksquare$ ).

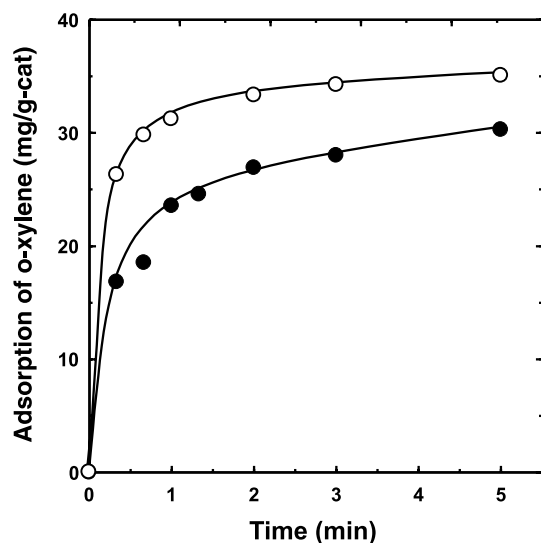


Figure 4. Adsorption kinetics of *o*-xylene over: nanosized mordenite sample ( $\text{SiO}_2/\text{Al}_2\text{O}_3 = 13.4$ ) ( $\circ$ ) and commercial mordenite sample ( $\bullet$ ).

### 3.2. Cracking of cumene (IPB) and 1,3,5-triisopropylbenzene (1,3,5-TIPB)

In order to probe the reactivity of both internal and external acid sites of the catalysts, the catalytic cracking of aromatic compounds including relatively small IPB and bulkier 1,3,5-TIPB was carried out over the MOR samples. As seen in table 2, the conversions of IPB are comparable for these two catalysts indicating they are indeed active solid acid catalysts. However, the nanosized MOR sample exhibits very low catalytic activity (10.9%) for the cracking of

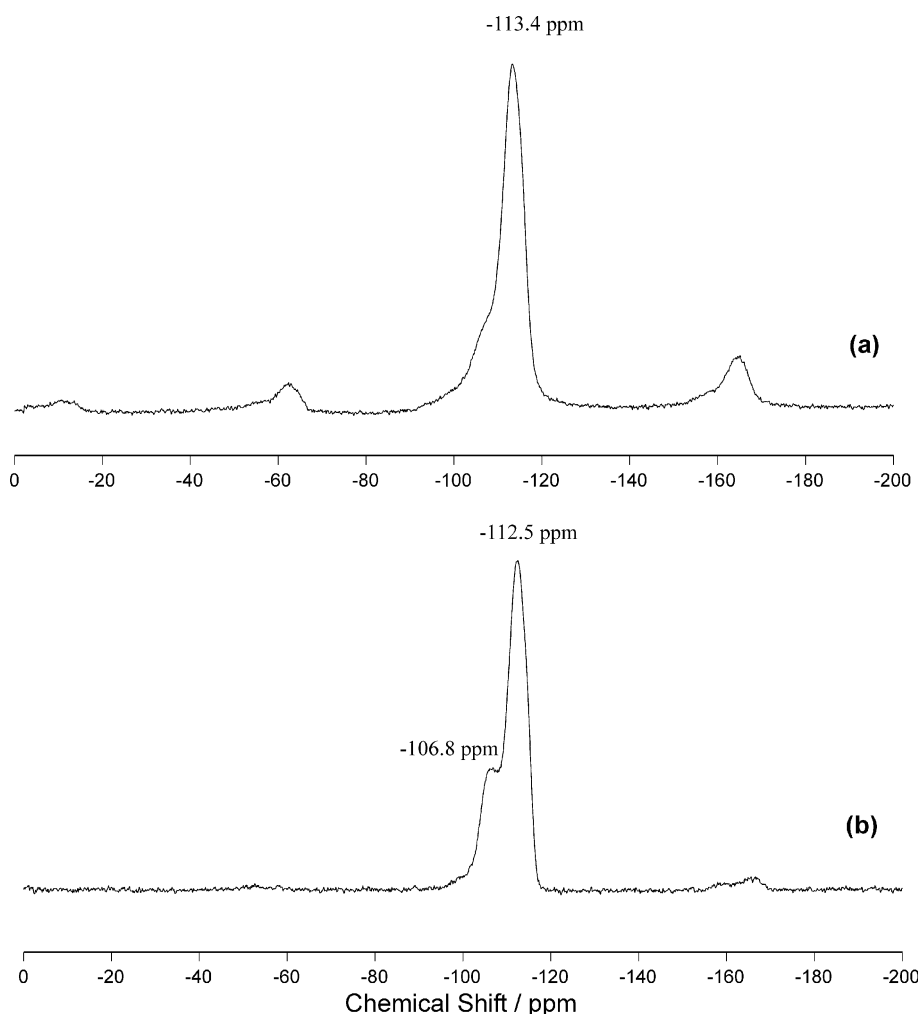


Figure 5.  $^{29}\text{Si}$  MAS NMR spectra of: (a) nanosized mordenite sample ( $\text{SiO}_2/\text{Al}_2\text{O}_3 = 13.4$ ) and (b) commercial mordenite sample ( $\text{SiO}_2/\text{Al}_2\text{O}_3 = 18.7$ ).

bulkier 1,3,5-TIPB compared to the commercial MOR sample (89.7%). The difference in the catalytic cracking of 1,3,5-TIPB might be due to a low density of acid sites on the external surface of the nanosized MOR sample compared to the commercial MOR sample. Since the size of IPB is small enough to enter the MOR type zeolite pores, we can reasonably conclude that the cracking of IPB indeed occurred inside the pores of the nanosized MOR catalyst.

### 3.3. Isopropylation of biphenyl

Figure 7 shows the conversions and the product selectivities of the isopropylation of biphenyl over the nanosized MOR sample ( $\text{SiO}_2/\text{Al}_2\text{O}_3 = 13.4$ ) and the commercial MOR sample ( $\text{SiO}_2/\text{Al}_2\text{O}_3 = 18.7$ ) as a function of temperature. At all reaction temperatures studied, the biphenyl conversions are comparable for these two catalysts. It is evident that the conversion of biphenyl increases rapidly as the temperature is increased from 200 to 300 °C and thereafter only a

marginal increase in the conversion of biphenyl is observed up to 350 °C. At lower temperatures, the 4,4'-DIPB and 4-IPBP are the predominant products and the amounts of 3,4'-DIPB and 3-IPBP are small in both cases. The selectivities to 4,4'-DIPB and 4-IPBP remain constant up to 250 °C. From the product distribution, it is seen that the selectivity for 4,4'-DIPB is dependent on temperature. At higher temperatures, the selectivity for 4,4'-DIPB decreases due to the isomerization of 4,4'-DIPB to the more thermodynamically stable 3,4'-DIPB. The selectivities of 4,4'-DIPB and 4-IPBP are found to be about 10% lower compared to the commercial MOR sample. It is pertinent to mention here that nanosized MOR sample should show higher catalytic activity for the isopropylation of biphenyl than the commercial MOR sample due to its high external surface area. However, due to the lower external surface activity of the nanosized MOR sample (section 3.2), the biphenyl conversions are comparable for both samples under the reaction conditions used in the present study.

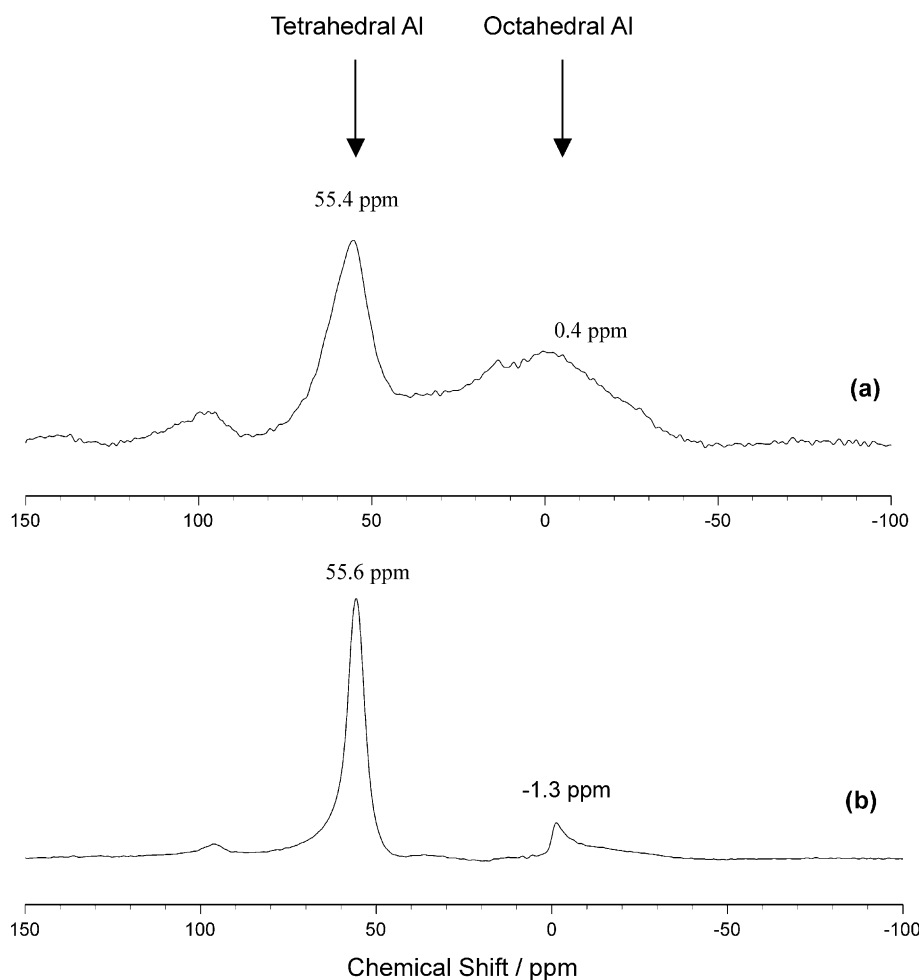


Figure 6.  $^{27}\text{Al}$  MAS NMR spectra of: (a) nanosized mordenite sample ( $\text{SiO}_2/\text{Al}_2\text{O}_3 = 13.4$ ) and (b) commercial mordenite sample ( $\text{SiO}_2/\text{Al}_2\text{O}_3 = 18.7$ ).

Table 2  
Cracking of cumene (IPB) and 1,3,5-triisopropylbenzene (1,3,5-TIPB) over mordenite catalysts<sup>a</sup>

Catalyst	Conversion (%)	
	IPB	1,3,5-TIPB
H-Mordenite ( $\text{SiO}_2/\text{Al}_2\text{O}_3 = 13.4$ ) <sup>b</sup>	96.1	10.9
H-Mordenite ( $\text{SiO}_2/\text{Al}_2\text{O}_3 = 18.7$ ) <sup>c</sup>	89.1	89.7

<sup>a</sup>Reaction conditions: catalyst = 10 mg, temperature = 400 °C.

<sup>b</sup>Sample obtained from Na-magadiite.

<sup>c</sup>Commercial sample (Tosoh Corporation, Tokyo, Japan).

than larger particles, they should allow easy access to the active sites by the reactants. Therefore, a higher conversion of 4,4'-DIPB is reasonably expected over the nanosized MOR sample than that over the commercial MOR sample. However, the isomerization of 4,4'-DIPB over the nanosized MOR sample is considerably lower than the commercial MOR sample in the temperature range of 250–350 °C. The difference in catalytic activity might be related to the presence of extra-framework aluminum species on the external surface and the lower acidity of the nanosized MOR sample.

### 3.4. Isomerization of 4,4'-DIPB

Furthermore, the isomerization of 4,4'-DIPB has also been carried out over both the catalysts at different temperatures by keeping the propylene pressure (0.8 MPa) constant. The results on the isomerization of 4,4'-DIPB over the nanosized MOR and the commercial MOR samples are shown in figure 8. Since nanosized particles have a much higher external surface

### 4. Conclusions

In conclusion, MOR type zeolite has been synthesized by hydrothermal transformation of Na-magadiite at 175 °C using TEAOH as the intercalating and/or structure directing agent. SEM reveals that the MOR crystallites obtained from Na-magadiite are of submicron size (0.1  $\mu\text{m}$ ). The catalytic activity of the nanosized MOR sample obtained from Na-magadiite

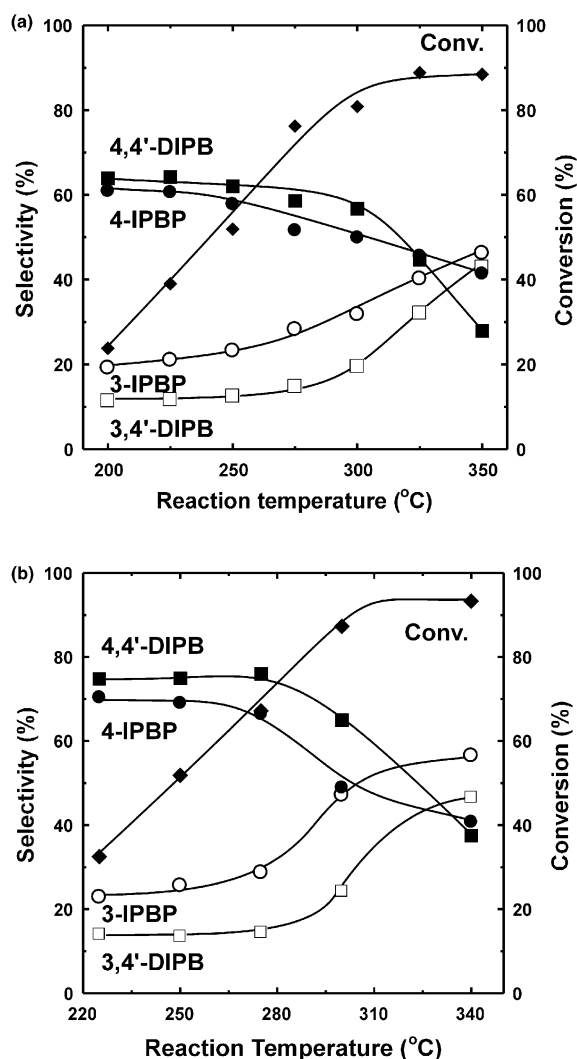


Figure 7. Effect of reaction temperature on the isopropylation of biphenyl with: (a) nanosized H-mordenite ( $\text{SiO}_2/\text{Al}_2\text{O}_3 = 13.4$ ) sample and (b) commercial H-mordenite sample ( $\text{SiO}_2/\text{Al}_2\text{O}_3 = 18.7$ ). Reaction conditions: biphenyl/catalyst =  $200 \text{ mmol g}^{-1}$ , propylene = 0.8 MPa, time = 4 h.

in the isopropylation reaction of biphenyl is comparable with that of a commercial MOR sample. The selectivities to 4,4'-DIPB and 4-IPBP, however, are about 10% lower on the nanosized MOR sample under similar reaction conditions. The reasons for the differences in catalytic activity of the nanosized MOR sample are: the presence of extra framework aluminum species and also the lower acidity in comparison to the commercial MOR sample.

#### Acknowledgment

W.S. thanks the Deutsche Forschungsgemeinschaft (Schw 478) and the Fonds der Chemischen Industrie (FCI) for generous financial assistance.

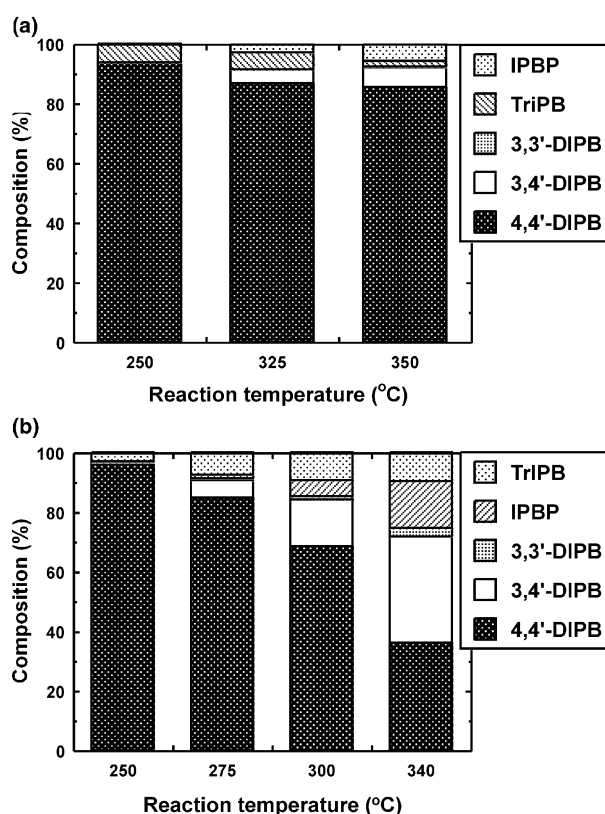


Figure 8. Effect of temperature on the isomerization of 4,4'-DIPB using: (a) nanosized H-mordenite ( $\text{SiO}_2/\text{Al}_2\text{O}_3 = 13.4$ ) sample and (b) commercial H-mordenite sample ( $\text{SiO}_2/\text{Al}_2\text{O}_3 = 18.7$ ). Reaction conditions: 4,4'-DIPB/catalyst =  $200 \text{ mmol g}^{-1}$ , propylene = 0.8 MPa, time = 4 h.

#### References

- [1] R.M. Gaydos, in: *Kirk-Othmer Encyclopedia of Chemical Technology*, 4th, ed., Vol. 4, eds. R.E. Kirk and D.F. Othmer (Wiley, New York, 1999) p. 232.
- [2] D.B. Priddy, *Ind. Eng. Chem., Prod. Res. Dev.* 8 (1969) 239.
- [3] T. Matsuda and E. Kikuchi, *Res. Chem. Inter.* 19 (1993) 319.
- [4] M. Matsumoto, Y. Suda, S. Yuzu and N. Kakihara, *PCT Int. Appl.* (1991) WO 9108181.
- [5] J.D. Fellmann, P.T. Lu, R.J. Saxton, P.R. Wentreck, E.G. Derouane and P. Massiani, *PCT Int. Appl.* (1991) WO 9103443.
- [6] J. Aguilar, A. Corma, F.V. Melo and E. Sastre, *Catal. Today* 55 (2000) 225.
- [7] Y. Sugi, Y. Kubota, T. Hanaoka and T. Matsuzaki, *Catal. Surv. Jpn.* 5 (2001) 43.
- [8] D. Mravec, J. Horniakova, P. Moreau and J. Joffre, *Petrol. Coal* 43 (2001) 107.
- [9] D.M. Roberge and W.F. Hoelderich in: *Zeolites and Mesoporous Materials at the Dawn of the 21st Century, Studies in Surface Science and Catalysis*, Vol. 135, eds. A. Galarneau, F. Di Renzo, F. Fajula and J. Vedrine (Elsevier, Amsterdam, 2001) p. 4161.
- [10] Y. Sugi, S. Tawada, T. Sugimura, Y. Kubota, T. Hanaoka, T. Matsuzaki, K. Nakajima and K. Kunimori, *Appl. Catal. A: Gen.* 189 (1999) 251.
- [11] M. Bandyopadhyay, R. Bandyopadhyay, S. Tawada, Y. Kubota and Y. Sugi, *Appl. Catal. A* 225 (2002) 51.
- [12] G.S. Lee, J.J. Maj, S.C. Rocke and J.M. Garces, *Catal. Lett.* 2 (1989) 234.

- [13] X. Tu, M. Matsumoto, T. Matsuzaki, T. Hanaoka, Y. Kubota, J.H. Kim and Y. Sugi, *Catal. Lett.* 21 (1993) 71.
- [14] Y. Sugi, T. Matsuzaki, T. Hanaoka, Y. Kubota, J.H. Kim, X. Tu and M. Matsumoto, *Catal. Lett.* 26 (1994) 181.
- [15] Y. Sugi, X. Tu, T. Matsuzaki, T. Hanaoka, Y. Kubota, J.H. Kim, M. Matsumoto, K. Nakajima and A. Igarashi, *Catal. Today* 31 (1996) 3.
- [16] D. Vergani, R. Prins and H.W. Kouwenhoven, *Appl. Catal. A* 163 (1997) 71.
- [17] D. Mravec, M. Michvocik and M. Hronec, *Petrol. Coal* 40 (1998) 44.
- [18] M. Sugimoto, H. Katsuno, K. Takatsu and N. Kawata, *Zeolites* 7 (1987) 503.
- [19] M. Yamamura, K. Chaki, T. Wakatsuki and K. Fujimoto, *Zeolites* 14 (1994) 643.
- [20] T. Selvam and W. Schwieger, in: *Studies in Surface Science and Catalysis*, Vol. 135, eds. A. Galarneau, F. Di Renzo, F. Fajula and J. Viedrine (Elsevier, Amsterdam, 2001) p. 411.
- [21] T. Selvam and W. Schwieger, in: *Impact of Zeolites and Other Porous Materials on the New Technologies at the Beginning of the New Millennium, Studies in Surface Science and Catalysis*, Vol. 142, Part A, eds. R. Aiello, G. Giordano and F. Testa (Elsevier, Amsterdam, 2002) p. 407.
- [22] G.J. Kim and W.S. Ahn, *Zeolites* 11 (1991) 745.
- [23] P. Luca, F. Crea, F. Fonseca and J.B. Nagy, *Micropor. Mesopor. Mater.* 42 (2001) 37.
- [24] B.O. Hincapie, L.J. Garces, Q. Zhang, A. Sacco and S.L. Suib, *Micropor. Mesopor. Mater.* 67 (2004) 19.
- [25] S. Tawada, Y. Sugi, Y. Kubota, Y. Imada, T. Hanaoka, T. Matsuzaki, K. Nakajima, K. Kunitomi and J.-H. Kim, *Catal. Today* 60 (2000) 243.
- [26] W. Schwieger, W. Heyer and K.-H. Bergk, *Z. Anorg. Allg. Chem.* 559 (1988) 191.
- [27] J.S. Dailly and T.J. Pinnavaia, *J. Incl. Phen. Mol. Recog. Chem.* 13 (1992) 47.
- [28] W.M. Meier, *Z. Kristallogr.* 115 (1961) 439.
- [29] W. Schwieger, M. Rauscher, R. Mönning, F. Scheffler and D. Freude in: *Nanoporous Materials II, Studies in Surface Science and Catalysis*, Vol. 129 eds. A. Sayari, M. Jaroniec and T.J. Pinnavaia (Elsevier, Amsterdam, 2000) p. 121.